

UDC 539.3

INFLUENCE OF STIFFNESS PARAMETERS ON VIBRO-IMPACT DAMPER DYNAMICS**P.P. Lizunov****O.S. Pogorelova****T.G. Postnikova***Kyiv National University of Construction and Architecture
31, Povitroflotskyave., Kyiv, Ukraine, 03680*

DOI: 10.32347/2410-2547.2023.110.21-35

The article studies the dynamic behavior of a low-mass vibro-impact damper, considered as a device for passive vibration control. Its design scheme corresponds to the scheme of single-sided vibro-impact nonlinear energy sink (SSVI NES), which is supposed to be used for effective vibrations attenuation under different transient loads, namely, impulsive, broadband, wind. Its dynamics and effectiveness strongly depend both on the damper own parameters and the external load parameters. We consider the response regimes and the damper efficiency for two options of its optimized parameters under periodic loading. The influence of the elasticity characteristics of the colliding surfaces on the damper effectiveness is also analyzed. We show that the modes with rich complex dynamics are implemented in a system with a heavier damper with low stiffness. Despite this, it is more effective, especially with a softer impact.

Keywords: vibro-impact, primary structure, damper, nonlinear energy sink, stiffness, elasticity.

1. Introduction

For many years, scientists and engineers have been studying the application of dynamic and impact dampers to mitigate vibrations. In recent decades, nonlinear sinks (NES) have come to be regarded as vibration control passive devices [1]. NES is a low-mass damper coupled with the main body – primary structure, which due to its nonlinearity, can absorb part of main body energy, that is, mitigate its vibrations. The author of article [2] determines the nonlinear energy sink as a single-degree-of-freedom (SDOF) structural element with relatively small mass and weak dissipation, attached to a primary structure via essentially nonlinear coupling. The world scientists have carried out many analytical, numerical and experimental investigations of NES; they hope to use these devices to mitigate vibrations, in particular, in high-rise buildings under the action of impulse, wind and even seismic loads. Numerous works on this topic demonstrate the active development of NES researches in recent years. There are comprehensive reviews of state-of-the-art researches on NESs [3-6], monographs [7, 8], dissertations [9, 10] and many articles on this problem [11-14]. Various types of NESs are being investigated; single-sided and double-sided vibro-impact NES (SSVI and DSVI) are one of them. The VI NESs consist of an oscillator and viscous damping elements, which can hit one or two obstacles rigidly connected to the primary structure.

It is believed in the literature that such a study can be divided into two sub-problems, namely the influences of parameters on the occurrence of response regimes and the efficiency of different response regimes [10]. Tightly relation of the device efficiency to response regimes conditions this division. Then the problem of parameters design optimization arises. Moreover, perhaps, the optimization mechanisms are not the same for different excitations. The author [10] emphasizes that a feasible and precise design of VI NES to control vibrations of nonlinear systems will be difficult, despite the fact that preliminary experimental results demonstrate good reduction of velocity and, therefore, the effectiveness of energy reduction.

Most authors describe the impact obtaining the relation between after and before impact under the hypothesis of the simplified shock theory and the condition of total momentum conservation. This theory considers the impact as instantaneous; it uses the restitution coefficient, which characterizes the elastic properties of the colliding surfaces. This coefficient is one of the damper parameters, and its effect on the VI NES efficiency is studied in many articles [10, 11, 15]. For example, in [16], the authors claim that the performance of the enhanced SSVI NES of nearly 0.45 (instead of common value of 0.7) coefficient of restitution is found to be more robust to the initial impulsive energy levels and to its physical parameters variation. The author of [10] believes that “an intermediate value will be optimal”. However, there are other ways of describing the impact in the scientific literature. In [17], purely elastic collisions are simulated by the Dirac delta function with a restitution coefficient equal to unity. A finite contact duration model of a VI NES is proposed in [18]. The authors examine three models, namely Hertz, Tsuji, and Kuwabara models, in which the contact impact force is presented as a nonlinear function of deformation. They compare and discuss the system dynamics implemented using both finite and instantaneous contact models. When considering the protection of a civil engineering frame structure against seismic events, the authors reveal a significant effect of the contact duration on the estimation of the dissipated energy, even for very brief collisions. Instantaneous contact model provides incommensurate values in terms of acceleration during the impacts, leading to a higher sensitivity to initial conditions revealed by large fluctuations of the mechanical response. On the contrary, it turns out that any finite duration contact models are less sensitive to initial conditions and, therefore, more accurate.

In this paper, we assume that the impact has a finite duration and model it applying Hertz's quasi-static contact theory, which takes into account the elastic properties of the contacting surfaces using Young's moduli of elasticity and Poisson's ratios. This is what makes it possible to analyze in more detail the influence of the damper elastic properties on the system dynamics.

In this paper, we continue the study of the SSVI NES dynamic behavior, started in our previous papers [19-21]. We consider two options of optimized damper parameters and response regimes implemented in the system. Complex oscillatory modes with rich dynamics that arise in the system for a certain

parameters set are considered. The effectiveness of the vibro-impact damper is also analyzed.

Thus, the goals of this paper are:

- determine the optimal damper parameters ensuring its maximal efficiency;
- analyze the response regimes that occur in the system with these parameters;
- analyze the influence of the elasticity characteristics of the colliding surfaces on the damper efficiency;
- show the best option for damper parameters.

2. Mathematical model

We consider two-body 2-DEF vibro-impact system, the calculating scheme of which corresponds to the model of single-sided vibro-impact nonlinear energy sink (SSVI NES) (Fig. 1) [9, 19].

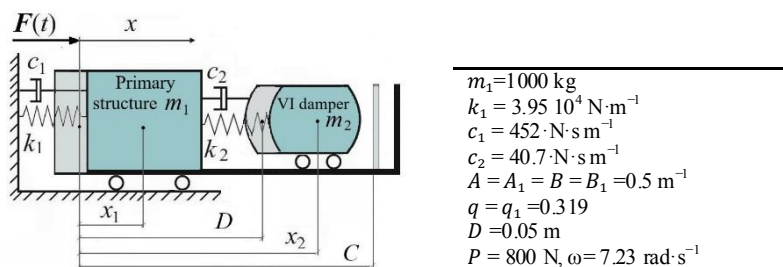


Fig. 1. Calculation scheme of SSVI NES

The primary structure of the mass m_1 is attached to a fixed wall by a linear elastic spring with a stiffness k_1 and a damper with a damping coefficient c_1 . A vibro-impact damper of much smaller mass m_2 is coupled with the primary structure by a linear elastic spring with a stiffness k_2 and a damper with a damping coefficient c_2 . The base, along which the damper moves without friction, is rigidly connected to the primary structure and has a barrier at its right end. The bodies coordinates are x_1 and x_2 ; the zero mark of the x -axis is at the primary structure mass center in an equilibrium state when all springs are not deformed. The initial distance between the bodies, that is, the length of the undeformed right spring, is equal to D . The distance to the right movable wall is C ; this distance defines the clearance (Fig. 1).

The motion equations for this system are as follows:

$$\begin{aligned}
 m_1 \ddot{x}_1 + c_1 \dot{x}_1 + k_1 x_1 - c_2 (\dot{x}_2 - \dot{x}_1) - k_2 (x_2 - x_1 - D) &= F(t) - H(z) F_{con}(z) + H(z_1) F_{con}(z_1), \\
 m_2 \ddot{x}_2 + c_2 (\dot{x}_2 - \dot{x}_1) + k_2 (x_2 - x_1 - D) &= +H(z) F_{con}(z) - H(z_1) F_{con}(z_1).
 \end{aligned} \quad (1)$$

The initial conditions are:

at $t=0$ we have

$$x_1(0) = 0, x_2(0) = D, \dot{x}_1(0) = 0, \dot{x}_2(0) = 0, \varphi_0 = 0. \quad (2)$$

In this article, we consider the system dynamic behavior under the action of an exciting harmonic force $F(t) = P \cos(\omega t + \varphi_0)$ with period $= 2\pi/\omega$.

Although the action of other exciting forces – impulsive, random, broadband, wind, is also subject to study [19].

In Eq.(1), $H(z)$ is the Heaviside step function $H(z) = \begin{cases} 1, & z \geq 0 \\ 0, & z < 0 \end{cases}$, it “actuates” the impact contact force $F(z)$ that acts only during an impact and simulates it. After our previous studying in [22], we consider it as nonlinear and write it in accordance with Hertz’s contact quasi-static theory [23]. The consideration of system calculation scheme in Fig.1 gives an understanding of the fact that the damper can hit both the left body directly and the obstacle rigidly connected with it. Therefore, the contact force at impact between bodies has the following form:

$$F_{con}(z) = K[z(t)]^{3/2}, \quad K = \frac{4}{3} \frac{q}{(\delta_1 + \delta_2)\sqrt{A+B}}, \quad \delta_1 = \frac{1-\nu_1^2}{E_1\pi}, \quad \delta_2 = \frac{1-\nu_2^2}{E_2\pi}, \quad (3)$$

and the same form for the impact of the damper on the right barrier:

$$F_{con}(z_1) = K_1[z_1(t)]^{3/2}, \quad K_1 = \frac{4}{3} \frac{q_1}{(\delta_3 + \delta_4)\sqrt{A_1+B_1}}, \quad \delta_3 = \frac{1-\nu_3^2}{E_3\pi}, \quad \delta_4 = \frac{1-\nu_4^2}{E_4\pi}. \quad (4)$$

Here $\nu_1, \nu_2, \nu_3, \nu_4$ are Poisson’s ratios; E_1, E_2, E_3, E_4 are Young’s moduli of elasticity for fourth colliding surfaces; A, A_1, B, B_1, q, q_1 are constants characterizing the contact zones geometry. The absorber surfaces, both left and right, are assumed to be spherical with large radii R and R_1 ; the contact surfaces of the primary structure and the right obstacle are flat. Then $A = B = 1/2R$, $A_1 = B_1 = 1/2R_1$, $q = q_1 = 0.319$ as in the collision of a plane and a sphere. It is the moduli of elasticity and Poisson’s ratios that characterize the elastic properties of the colliding surfaces. Therefore, the analysis of their values should allow us to see the influence on the system dynamics in more detail than the analysis of the restitution coefficient.

The variables z and z_1 are the colliding bodies rapprochement upon impact, since the Hertz’s theory allows local deformations in the contact zone.

When an impact between the bodies occurs, then $x_1 \geq x_2$, i.e. $x_1 - x_2 \geq 0$. There is no impact when $x_1 < x_2$, i.e. $x_1 - x_2 < 0$. Then $z = x_1 - x_2$.

An impact of the damper on the obstacle occurs when $x_2 = x_1 + C$, i.e., $x_2 - x_1 = C$, i.e., $x_2 - x_1 - C = 0$. During impact $x_2 - x_1 - C \geq 0$. There is no impact when $x_2 - x_1 - C < 0$. Then $z_1 = x_2 - x_1 - C$. Clearance is $C - D$.

3. Damper parameters optimization

Dynamic behavior and efficiency of a vibro-impact damper strongly depend on the totality of its parameters. The primary structure parameters are set and cannot be changed. The totality of damper parameters includes its mass, stiffness, damping coefficient, clearance, restitution coefficient or other characteristics of the colliding surfaces elasticity. By optimizing in three parameters, we have set m_2 damper mass, k_2 stiffness and C clearance [21]. The optimization was carried out using the solver *fminsearch* (platform *MatLab*) and the solver *fmincon* (platform *Octave*). The optimal parameters should provide the maximal damper effectiveness, that is, the strongest mitigation of the primary structure vibrations; its oscillatory amplitude and velocity should be as low as possible. Initially, we choose low-mass damper with parameters $m_2 = 20$ kg, $k_2 = 3190$ N · m⁻¹, $C = 0.06$ m. Optimum damper settings allow

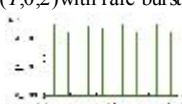
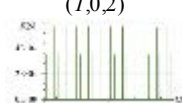
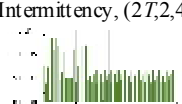
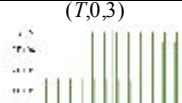
for improved vibration attenuation, as shown in Table 1. However, the 5 version ensures the worse mitigation than 3 and 4 versions, although it provides a periodic oscillatory mode with 3 impacts on an obstacle per cycle. The 6 version gives the worst mitigation, the movement is shockless, such damper is not nonlinear and is not interesting in this article.

Note. Following the logic of [24], we call the periodic mode of the kT -period with n damper impacts directly on the primary structure and m its impacts on an obstacle rigidly connected to the primary structure as (kT, n, m) .

Thus, we choose for consideration options 3 and 4 of optimized damper parameters. Option 4 provides the best mitigation, but the oscillatory regime is essentially irregular with the damper impacts both on the barrier and directly on the primary structure; its dynamics is rich and complex. Therefore, this regime is worth showing in detail; its characteristics are shown in Fig. 2, 3. In addition, the damper mass is almost 4% from the primary structure mass and its stiffness is too low. These circumstances should be taken into account when choosing the optimal damper. Note that when demonstrating the oscillatory mode implemented in the system, we show the time histories of the contact forces, drawing the forces in impacts on the barrier F_{conR} in green and in direct impacts on the primary structure F_{conL} in blue. It is these dependences that most clearly show the regime type, since the amplitudes change less during bursts, while the forces change strongly.

Table 1

The results of damper parameters optimization

№	m_2 , kg	k_2 , N/m	C , m	$A_{\text{max1},m}$ $V_{\text{max1},m} \cdot \text{s}^{-1}$	Wane %	Regime Time history of contact forces F_{conR}
1	0	0	0	0.0602 0.436		Without damper
2	20	3190	0.06	0.0557 0.401	7.5 8.0	$(T,0,2)$ with rare bursts 
3	22.67	2481.1	0.0683	0.0540 0.387	10.3 11.2	$(T,0,2)$ 
4	37.88	414.6	0.0747	0.0522 0.380	13.3 12.8	Intermittency, $(2T,2,4)$ 
5	19.85	3190	0.0564	0.0552 0.400	8.3 9.0	$(T,0,3)$ 

In Fig. 2, the general motion characteristics of regime for option 4 are shown. Intermittency with alternating periodic and chaotic phases is visible. The graph of the relative damper displacement, that is, the difference $(x_2 - x_1)$ (Fig. 2, b), demonstrates the impacts both on the obstacle at $(x_2 - x_1) = C = 0.0747$ m and on the primary structure directly at $(x_2 - x_1) = 0$. In the periodic phase, the contact forces during impacts between the bodies (F_{conL} , “blue” forces) are greater than during impacts against an obstacle (F_{conR} , “green” forces). During the bursts, the changes in amplitudes are not great (Fig. 2, a), but the changes in the contact forces are significant. Where the contact forces between bodies F_{conL} become larger (Fig. 2, c), the contact forces F_{conR} become smaller (Fig. 2, d), and vice versa.

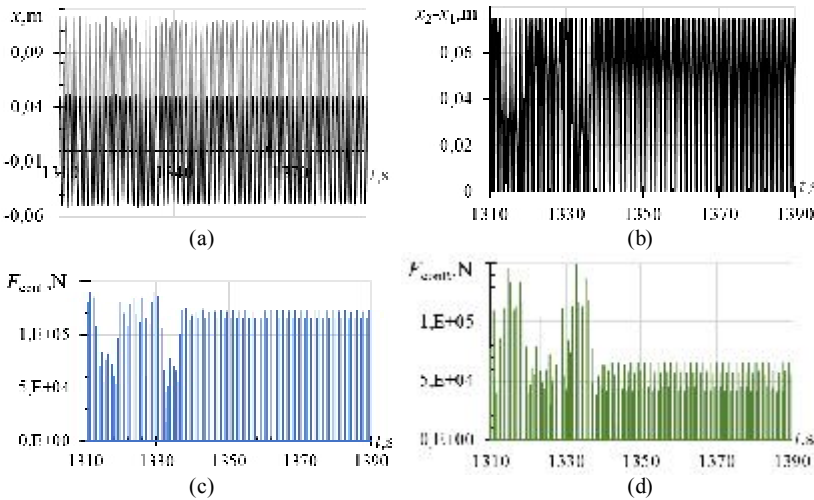


Fig. 2. The general motion characteristics of the system with damper parameters $m_2=37.88$ kg, $k_2=414.6$ N·m⁻¹, $C=0.0747$ m.

Since the motions in periodic and chaotic phases are, of course, completely different, we will show them in Fig. 3.

In the figures in the 1st row, small changes in the amplitudes are clearly visible. Graphs of the relative damper displacements in the 2nd row demonstrate impacts both against the primary structure directly and on the barrier. The time history of impact contact force in the right panel in the 3rd row shows two direct impacts on the primary structure and four impacts on the obstacle per cycle in $2T$. Phase trajectories with Poincaré maps for primary structure on the left and the damper on the right in the 4th row are typical for chaotic and almost periodic motion.

4. Influence of the characteristics of colliding surfaces elasticity during impacts on an obstacle

In many works in the world scientific literature [10, 11, 15, 16], the influence of the restitution coefficient r_c on vibration mitigation is studied. The

authors believe that its smaller value provides a better effect. A lower value of the restitution coefficient means a decrease in the impact elasticity and an increase in possible local deformations of the colliding surfaces. Therefore, in our problem formulation using nonlinear Hertzian force to describe the impact, it is advisable to reduce the values of Young's elasticity moduli and increase the Poisson's ratios for the colliding surfaces. This should provide a softer impact and larger local deformations of these surfaces. The results of such changes in these characteristics of the contacting surfaces elasticity are given in Table 2 and Table 3.

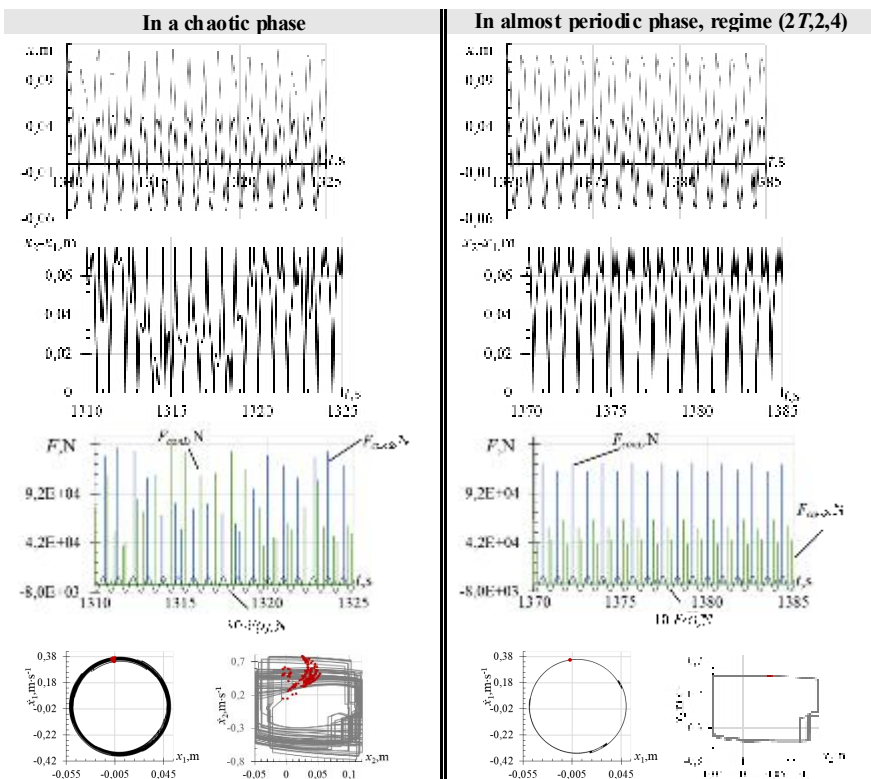


Fig. 3. Motion characteristics of the system with damper parameters $m_2=37.88$ kg, $k_2=414.6$ N·m⁻¹, $C=0.0747$ m in the chaotic and almost periodic phases of intermittency

A strong decrease in the elasticity modulus greatly reduces the impact contact force, by 28 times. The oscillatory regime becomes purely periodic with two impacts on the barrier per cycle without any bursts. Note, by the way, that in [10], the author advises to put the focus on the regime with two impacts per cycle of VI NES, since it is this regime that is important for vibration control. Increasing Poisson's ratios has no effect. However, these changes in the system dynamics with such damper parameters do not affect the values of the primary structure amplitudes and velocities. Such a strong decrease in the

contact force suggests the idea of checking the operation of a linear damper without any impacts. Indeed, in this case, the characteristics of the system oscillatory motion are as follows:

$$A_{\max 1} = 0.0517 \text{ m}, V_{\max 1} = 0.374 \text{ m s}^{-1}, A_{\max 2} = 0.0974 \text{ m}, V_{\max 2} = 0.705 \text{ m s}^{-1}.$$

Table 2

The influence of the characteristics of the colliding surfaces elasticity at impacts on an obstacle when damper parameters are:
 $m_2=22.67 \text{ kg}, k_2=2481.1 \text{ N}\cdot\text{m}^{-1}, C=0.0683 \text{ m}$

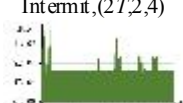
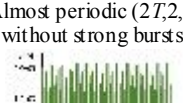
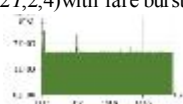
№	$E_3, E_4, \text{ N}\cdot\text{m}^{-2}$	v_3, v_4	$A_{\max 1}, \text{ m}$ $V_{\max 1}, \text{ m}\cdot\text{s}^{-1}$	Wane %	$A_{\max 2}, \text{ m}$ $V_{\max 2}, \text{ m}\cdot\text{s}^{-1}$	$F_{\text{conR}}, \text{ N}$	Regime
1	$2.1\cdot 10^{11}$ $2.1\cdot 10^{11}$	0.3 0.3	0.0540 0.387	10.3 11.2	0.0758 0.684	65619	(T,0,2) with rare bursts
2	$2.1\cdot 10^{11}$ $2.1\cdot 10^7$	0.3 0.3	0.0537 0.385	10.8 11.7	0.0760 0.678	1979	(T,0,2)
3	$2.1\cdot 10^{11}$ $2.1\cdot 10^7$	0.3 0.4	0.0537 0.385	10.8 11.7	0.0759 0.677	2040	(T,0,2)
4	$2.1\cdot 10^{11}$ $2.1\cdot 10^7$	0.3 0.49	0.0538 0.385	10.6 11.7	0.0758 0.676	2117	(T,0,2)
5	$2.1\cdot 10^7$ $2.1\cdot 10^7$	0.4 0.4	0.0537 0.385	10.8 11.7	0.0768 0.685	1584	(T,0,2)
6	$2.1\cdot 10^7$ $2.1\cdot 10^7$	0.49 0.49	0.0537 0.385	10.8 11.7	0.0766 0.684	1641	(T,0,2)

The mitigation of the primary structure vibrations is: 14.1% in amplitudes and 14.2% in velocities, which is slightly better than that of the vibro-impact damper. However, it is believed that the simplicity of the device and reliability of operation make shock absorbers suitable for use in tower buildings. At the same time, the use of the dynamic damper to protect buildings has the following disadvantages: firstly, the relative complexity of the damper design and, secondly, the impossibility of their use in mass construction due to the need to adjust individually the dampers for each specific building.

As in the previous case, a strong decrease in the elasticity modulus greatly reduces the impact contact force. The oscillatory regime becomes smoother and close to periodic only with rare bursts of irregular movement. But the damper impacts directly on the primary structure – four impacts per cycle in $2T$ – occur at all values of the elasticity modulus. It does not matter whether one or both of the elastic moduli decrease on two colliding surfaces. An increase in Poisson's ratios does not reduce the primary structure amplitudes, but it does affect the system dynamics. Comparing versions 5 and 6, we see changes in the values of contact force and damper velocity when changing only Poisson's ratios. The options 2 and 3 differ strongly when changing only one Poisson's ratio. However, these changes in the system dynamics with such damper parameters also do not affect the values of the primary structure amplitudes and velocities. Only option 2 is an exception. Why is it so?

Table 3

The influence of the characteristics of the colliding surfaces elasticity at impacts on an obstacle when damper parameters are: $m_2=37.88$ kg, $k_2=414.6$ N·m⁻¹, $C=0.0747$ m ($E_1=E_2=2.1 \cdot 10^{11}$ N·m⁻², $v_1=v_2=0.3$)

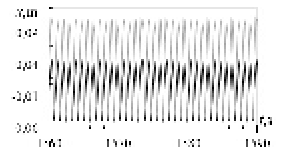
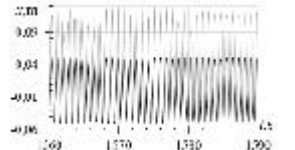
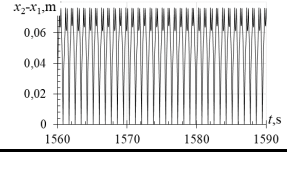
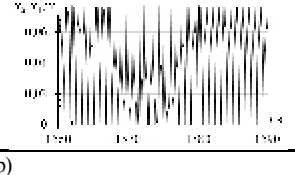

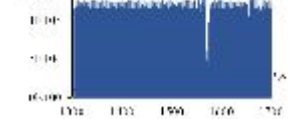
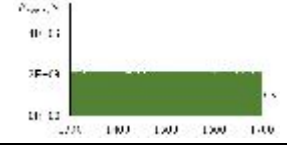
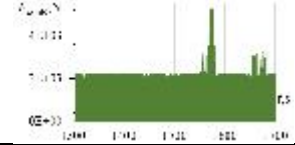
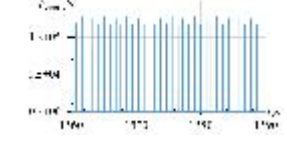
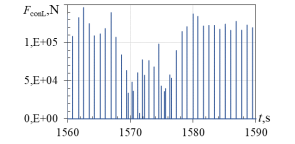
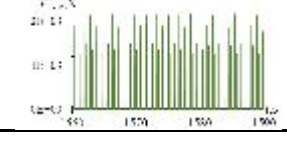
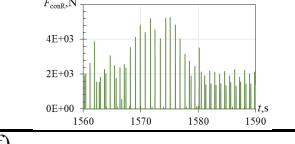
№	$\frac{E_3, E_4,}{\text{N} \cdot \text{m}^{-2}}$	v_3, v_4	$\frac{A_{\max 1},}{\text{m}}, \frac{V_{\max 1},}{\text{m} \cdot \text{s}^{-1}}$	Wane %	$\frac{A_{\max 2},}{\text{m}}, \frac{V_{\max 2},}{\text{m} \cdot \text{s}^{-1}}$	$F_{\text{conR}}, \text{N}$	Regime Time history of contact forces F_{conR}
1	$2.1 \cdot 10^{11}$ $2.1 \cdot 10^{11}$	0.3 0.3	0.0522 0.380	13.3 13.8	0.0878 0.783	149419	Intermit, (2T,2,4) 
2	$2.1 \cdot 10^{11}$ $2.1 \cdot 10^7$	0.3 0.3	0.0494 0.361	17.9 17.2	0.0851 0.530	2188	Almost periodic (2T,2,4) without strong bursts 
3	$2.1 \cdot 10^{11}$ $2.1 \cdot 10^7$	0.3 0.4	0.0518 0.379	14.0 13.1	0.0888 0.803	5262	(2T,2,4) with rare bursts 
4	$2.1 \cdot 10^{11}$ $2.1 \cdot 10^7$	0.3 0.49	0.0514 0.373	14.5 14.4	0.0885 0.761	5426	
5	$2.1 \cdot 10^7$ $2.1 \cdot 10^7$	0.4 0.4	0.0515 0.374	14.5 14.2	0.0882 0.673	2718	
6	$2.1 \cdot 10^7$ $2.1 \cdot 10^7$	0.49 0.49	0.0513 0.373	14.8 14.4	0.0885 0.749	3755	

Let us compare the system movement in options 2 and 3 in more detail (Table 4). The time histories of the bodies displacements are shown at level (a); the difference of displacements ($x_2 - x_1$), i.e. the relative damper displacement – at level (b). Time histories of the contact forces at direct impacts on the primary structure are shown in blue at level (c) and on the obstacle in green at level (d); time histories of the same forces are shown on an enlarged scale at levels (e) and (f).

It is worth paying attention to the graphs of the relative damper displacements at level (b). They show both direct impacts between bodies, when $(x_2 - x_1) = 0$, and the damper impacts on an obstacle, when $(x_2 - x_1) = C = 0.0747$ m. It should be noted that the contact forces with direct impacts between bodies are greater than with the damper impacts against an obstacle. During the bursts, there, where “green” forces increase, “blue” forces decrease and vice versa.

The regime for option 2 shown on the left panel is not periodic, but it is entirely smooth without strong bursts of irregular motion. On the contrary, the mode for option 3 on the right panel has although rare but strong bursts. It is due to these bursts that the maximum value of the amplitude increases, since it is much smaller on a smooth section.

Table 4
The comparison of system dynamics for options 2 and 3 from Table 3

Option 2	Option 3	Note for option 3
		<p>On smooth region without bursts $1300 \text{ s} \leq t \leq 1500 \text{ s}$ $A_{\max 1} = 0.0494 \text{ m}$ $V_{\max 1} = 0.360 \text{ m} \cdot \text{s}^{-1}$ $A_{\max 2} = 0.0851 \text{ m}$ $V_{\max 2} = 0.529 \text{ m} \cdot \text{s}^{-1}$</p>
(a)		
		<p>On all region with bursts $1300 \text{ s} \leq t \leq 1700 \text{ s}$ $A_{\max 1} = 0.0518 \text{ m}$ $V_{\max 1} = 0.379 \text{ m} \cdot \text{s}^{-1}$ $A_{\max 2} = 0.0888 \text{ m}$ $V_{\max 2} = 0.803 \text{ m} \cdot \text{s}^{-1}$</p>
(b)		
		
(c)		
		<p>On smooth region without bursts $1300 \text{ s} \leq t \leq 1500 \text{ s}$ $F_{\text{conL}} = 127795 \text{ N}$ $F_{\text{conR}} = 2257 \text{ N}$</p>
(d)		
		<p>On all region with bursts $1300 \text{ s} \leq t \leq 1700 \text{ s}$ $F_{\text{conL}} = 146148 \text{ N}$ $F_{\text{conR}} = 5262 \text{ N}$</p>
(e)		
		
(f)		

Thus, we can state that a heavier damper with low stiffness and a softer impact on the obstacle mitigates the primary structure vibrations more strongly, despite the irregular motion modes. Rare bursts of irregular motion within the periodic one worsen the mitigation. And although in one case (in option 2) a motion without strong bursts was obtained, we cannot indicate a

recipe for such a movement implementation, since in all other cases there are rare strong bursts.

The presence of direct impacts on the primary structure, along with impacts on the barrier, suggests an idea about a double-sided VNES. However, let's see how the type of this impact affects the system dynamics.

5. Influence of the characteristics of the colliding surfaces elasticity during direct impacts on the primary structure

The impact softening for impacts both on the primary structure and on a barrier gave good results as shown in Table 5 for the system with damper parameters $m_2=37.88$ kg, $k_2=414.6$ N·m⁻¹, $C=0.0747$ m.

Table 5

The influence of the characteristics of the colliding surfaces elasticity at impacts both on the primary structure directly and on an obstacle
 $m_2=37.88$ kg, $k_2=414.6$ N·m⁻¹, $C=0.0747$ m

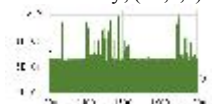
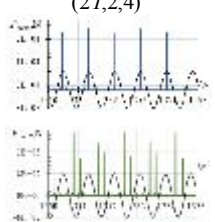
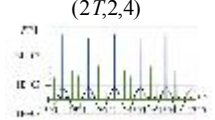
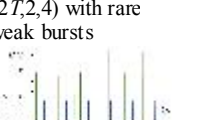
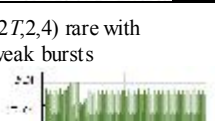

№	$E_1, E_2,$ $E_3, E_4,$ N·m ⁻²	v_1 v_2 v_3 v_4	$A_{max1},$ m $V_{max1},$ m·s ⁻¹	Wane %	$A_{max2},$ m $V_{max2},$ m·s ⁻¹	$F_{conL},$ $F_{conR},$ N	Regime Time history of contact forces
1	$2.1 \cdot 10^{11}$ $2.1 \cdot 10^7$ $2.1 \cdot 10^{11}$ $2.1 \cdot 10^{11}$	0.3 0.49 0.3 0.3	0.0532 0.386	11.6 11.5	0.0890 0.787	5351 150339	Intermittency, (2T,2,4) 
2	$2.1 \cdot 10^{11}$ $2.1 \cdot 10^9$ $2.1 \cdot 10^{11}$ $2.1 \cdot 10^7$	0.3 0.35 0.3 0.49	0.0493 0.360	18.1 17.4	0.0850 0.527	26830 2343	(2T,2,4) 
3	$2.1 \cdot 10^{11}$ $2.1 \cdot 10^7$ $2.1 \cdot 10^{11}$ $2.1 \cdot 10^7$	0.3 0.49 0.3 0.49	0.0492 0.358	18.3 17.9	0.0851 0.532	4505 2359	(2T,2,4) 
4	$2.1 \cdot 10^{11}$ $2.1 \cdot 10^7$ $2.1 \cdot 10^{11}$ $2.1 \cdot 10^9$	0.3 0.49 0.3 0.3	0.0493 0.360	18.1 17.4	0.0851 0.533	4482 13851	(2T,2,4) with rare weak bursts 
5	$2.1 \cdot 10^{11}$ $2.1 \cdot 10^7$ $2.1 \cdot 10^{11}$ $2.1 \cdot 10^9$	0.3 0.49 0.3 0.4	0.0497 0.365	17.4 16.3	0.0862 0.582	4884 15406	(2T,2,4) rare with weak bursts 
6	$2.1 \cdot 10^{11}$ $2.1 \cdot 10^7$ $2.1 \cdot 10^{11}$ $2.1 \cdot 10^9$	0.3 0.49 0.3 0.49	0.0493 0.359	18.1 17.7	0.0850 0.530	4470 14858	

Table 5 shows that a decrease in the elastic moduli of the colliding surfaces both for left and right impacts gives fairly stable results. This softening of impacts reduces the contact forces, smoothes the motion, making it purely periodic or periodic with rare weak bursts, and provides a decrease in the primary structure amplitudes and velocities by about 18%. Thus, we can probably consider that in this case the single-sided VI NES has become a double-sided VI NES. However, the role of the left obstacle is the primary structure itself.

It is worth noting an unexpected result for a damper without a right obstacle, when impacts occur only on the primary structure. Table 6 shows the gain of the primary structure vibrations by about 13%, which occurs due to the huge contact force during impacts between the bodies.

Table 6

Increase in vibrations of the primary structure in absence of the right obstacle for damper parameters $m_2 = 37.88$ kg, $k_2 = 414.6$ N·m⁻¹, $C = 0.0747$ m

$E_1, E_2, \text{N}\cdot\text{m}^{-2}$	v_1, v_2	$A_{\max 1}, \text{m}$ $V_{\max 1}, \text{m}\cdot\text{s}^{-1}$	Rise %	$A_{\max 2}, \text{m}$ $V_{\max 2}, \text{m}\cdot\text{s}^{-1}$	$F_{\text{conL}}, \text{N}$	Regime Time history of contact forces F_{conL}
		0.0602 0.436				Without damper
$2.1 \cdot 10^{11}$ $2.1 \cdot 10^{11}$	0.3 0.3	0.0685 0.494	13.8 13.3	0.121 0.828	223793	(T,1,0) with rare weak bursts

8. Conclusions

An analysis of the dynamic behavior of a vibro-impact system with a damper made it possible to draw the following conclusions. The calculation scheme of the system, consisting of the primary structure and the damper attached to it, corresponds to the scheme of single-sided vibro-impact nonlinear sink (SSVI NES).

- The optimization of the damper parameters has identified two options that provide its greatest efficiency, that is, the strongest reduction in the primary structure oscillatory amplitudes and velocities.

- A heavier damper with small stiffness ensures stronger vibrations mitigation. However, the oscillatory regimes in this case are irregular with complex dynamics. The damper hits not only an obstacle rigidly connected to the primary structure, but also directly into the primary structure.

- Reducing the moduli of elasticity in both impacts, that is, impacts softening, smoothes the oscillatory regimes, making them almost periodic, and increases the damper effectiveness. The single-sided VI NES in this case becomes a double-sided VI NES, but the second obstacle is the primary structure itself.

- The dynamics of a system with SSVI NES, like any strongly nonlinear discontinuous system, is sensitive to changes in its parameters, even small changes.

REFERENCES

1. Ding, H., & Chen, L.-O. (2020). Designs, analysis, and applications of nonlinear energy sinks. *Nonlinear Dynamics*, 100(4), 3061–3107. <https://doi.org/10.1007/s11071-020-05724-1>
2. Gendelman, O. V. (2012). Analytic treatment of a system with a vibro-impact nonlinear energy sink. *Journal of Sound and Vibration*, 331(21), 4599–4608. <https://doi.org/10.1016/j.jsv.2012.05.021>
3. Vakakis, A. F. (2018). Passive nonlinear targeted energy transfer. *Philosophical Transactions of the Royal Society A: Mathematical, Physical and Engineering Sciences*, 376(2127), 20170132. <https://doi.org/10.1098/rsta.2017.0132>
4. Lu, Z., Wang, Z., Masri, S. F., & Lu, X. (2017). Particle impact dampers: Past, present, and future. *Structural Control and Health Monitoring*, 25(1), e2058. <https://doi.org/10.1002/stc.2058>
5. Ibrahim, R. A. (2008). Recent advances in nonlinear passive vibration isolators. *Journal of Sound and Vibration*, 314(3–5), 371–452. <https://doi.org/10.1016/j.jsv.2008.01.014>
6. Saeed, A. S., Abdul Nasar, R., & AL-Shudeifat, M. A. (2022). A review on nonlinear energy sinks: designs, analysis and applications of impact and rotary types. *Nonlinear Dynamics*, 111(1), 1–37. <https://doi.org/10.1007/s11071-022-08094-v>
7. Lee, Y. S., Vakakis, A. F., Bergman, L. A., McFarland, D. M., Kerschen, G., Nucera, F., Tsakirtzis, S., & Panagopoulos, P. N. (2008). Passive non-linear targeted energy transfer and its applications to vibration absorption: A review. *Proceedings of the Institution of Mechanical Engineers, Part K: Journal of MultiBody Dynamics*, 222(2), 77–134. <https://doi.org/10.1243/14644193jmbd118>
8. Wang, J., Wierschem, N. E., Spencer, B. F., & Lu, X. (2015). Track Nonlinear Energy Sink for Rapid Response Reduction in Building Structures. *Journal of Engineering Mechanics*, 141(1). [https://doi.org/10.1061/\(asce\)em.1943-7889.0000824](https://doi.org/10.1061/(asce)em.1943-7889.0000824)
9. Wierschem, N. E. (2014). Targeted energy transfer using nonlinear energy sinks for the attenuation of transient loads on building structures. University of Illinois at Urbana-Champaign.
10. Tao Li (2016). Study of nonlinear targeted energy transfer by vibro-impact. Doctorat de l'universite de Toulouse
11. Youssef, B., & Leine, R. I. (2021). A complete set of design rules for a vibro-impact NES based on a multiple scales approximation of a nonlinear mode. *Journal of Sound and Vibration*, 501, 116043. <https://doi.org/10.1016/j.jsv.2021.116043>
12. Bergeot, B., Bellizzi, S., & Berger, S. (2021). Dynamic behavior analysis of a mechanical system with two unstable modes coupled to a single nonlinear energy sink. *Communications in Nonlinear Science and Numerical Simulation*, 95, 105623. <https://doi.org/10.1016/j.cnsns.2020.105623>
13. Saeed, A. S., AL-Shudeifat, M. A., Cantwell, W. J., & Vakakis, A. F. (2021). Two-dimensional nonlinear energy sink for effective passive seismic mitigation. *Communications in Nonlinear Science and Numerical Simulation*, 99, 105787. <https://doi.org/10.1016/j.cnsns.2021.105787>
14. Luo, J., Wierschem, N. E., Hubbard, S. A., Fahnestock, L. A., Dane Quinn, D., Michael McFarland, D., Spencer, B. F., Vakakis, A. F., & Bergman, L. A. (2014). Large-scale experimental evaluation and numerical simulation of a system of nonlinear energy sinks for seismic mitigation. *Engineering Structures*, 77, 34–48. <https://doi.org/10.1016/j.engstruct.2014.07.020>
15. Li, W., Wierschem, N. E., Li, X., Yang, T., & Brennan, M. J. (2020). Numerical study of a symmetric single-sided vibro-impact nonlinear energy sink for rapid response reduction of a cantilever beam. *Nonlinear Dynamics*, 100(2), 951–971. <https://doi.org/10.1007/s11071-020-05571-0>
16. AL-Shudeifat, M. A., & Saeed, A. S. (2020). Comparison of a modified vibro-impact nonlinear energy sink with other kinds of NESs. *Meccanica*, 56(4), 735–752. <https://doi.org/10.1007/s11012-020-01193-3>
17. Farid, M. (2023). Dynamics of a hybrid cubic vibro-impact oscillator and nonlinear energy sink. *Communications in Nonlinear Science and Numerical Simulation*, 117, 106978. <https://doi.org/10.1016/j.cnsns.2022.106978>

18. Lo Feudo, S., Job, S., Cavallo, M., Fraddosio, A., Piccioni, M. D., & Tafuni, A. (2022). Finite contact duration modeling of a Vibro-Impact Nonlinear Energy Sink to protect a civil engineering frame structure against seismic events. *Engineering Structures*, 259, 114137. <https://doi.org/10.1016/j.engstruct.2022.114137>
19. Lizunov, P., Pogorelova, O., & Postnikova, T. (2022). Choice of the Model for Vibro-impact Nonlinear Energy Sink. *Strength of Materials and Theory of Structures*, 108, 63–76. <https://doi.org/10.32347/2410-2547.2022.108.63-76>
20. Lizunov, P., Pogorelova, O., & Postnikova, T. (2022). Dynamics of primary structure coupled with singlesided vibro-impact nonlinear energy sink. *Strength of Materials and Theory of Structures*, 109, 103–113. <https://doi.org/10.32347/2410-2547.2022.109.20-29>
21. Lizunov, P., Pogorelova, O., & Postnikova, T. (2023). Vibro-impact damper dynamics depending on system parameters. *Journal of Vibration Engineering & Technologies*. Current Status: Under Review. Preprint Research Square DOI: 10.21203/rs.3.rs-2786639/v1
22. Bazhenov, V., Pogorelova, O., & Postnikova, T. (2021). Crisis-Induced Intermittency and Other Nonlinear Dynamics Phenomena in Vibro-impact System with Soft Impact. *Nonlinear Mechanics of Complex Structures*, 185–203. https://doi.org/10.1007/978-3-030-75890-5_11
23. Johnson, K. L. (1985). *Contact Mechanics*. <https://doi.org/10.1017/cbo9781139171731>
24. Lamarque C. H., Janin O. (2000). Modal analysis of mechanical systems with impact nonlinearities: limitations to a modal superposition. *Journal of sound and vibration*. 235(4), 567-609. <https://doi.org/10.1006/jsvi.1999.2932>

Стаття надійшла 03.04.2023

Лізунов П.П., Погорелова О.С., Постнікова Т.Г.

ВПЛИВ ПАРАМЕТРІВ ЖОРСТКОСТІ НА ДИНАМІКУ ВІБРОУДАРНОГО ДЕМПФЕРА

В статті вивчається динамічна поведінка віброударного демпфера малої маси, який розглядається як засіб пасивного управління вібрацією. Його розрахункова схема відповідає схемі одностороннього віброударного нелінійного поглинача енергії (single-sided vibro-impact nonlinear energy sink – SSVI NES). Передбачається, що він може бути використаний для ефективного гасіння коливань при різному перехідному навантаженні, а саме, імпульсному, широко смугастому, вітровому. Його динаміка та ефективність сильно залежать як від власних параметрів демпфера, так і від параметрів зовнішнього навантаження. Режими реагування та ефективність демпфера розглядаються для двох варіантів його оптимізованих параметрів при періодичному навантаженні. Також аналізується вплив характеристик пружності контактуючих поверхонь на ефективність демпфера. Показано, що в системі з більш важким демпфером та з його невеликою жорсткістю реалізуються коливальні режими з багатою складною динамікою. Проте такий демпфер виявився ефективнішим, особливо при м'якшому ударі.

Ключові слова: віброударний, первинна структура, демпфер, нелінійний поглинач енергії, жорсткість, пружність

УДК 539.3

Лізунов П.П., Погорелова О.С., Постнікова Т.Г. Вплив параметрів жорсткості на динаміку віброударного демпфера // Опір матеріалів і теорія споруд: наук.-тех. збірн. – К.: КНУБА. 2023. – Вип. 110. – С. 21-35. – Англ.

В статті вивчається динамічна поведінка віброударного демпфера малої маси, який розглядається як засіб пасивного управління вібрацією. Його розрахункова схема відповідає схемі одностороннього віброударного нелінійного поглинача енергії (single-sided vibro-impact nonlinear energy sink – SSVI NES). Передбачається, що він може бути використаний для ефективного гасіння коливань при різному перехідному навантаженні, а саме, імпульсному, широко смугастому, вітровому. Його динаміка та ефективність сильно залежать як від власних параметрів демпфера, так і від параметрів зовнішнього навантаження. Режими

резування та ефективність демпфера розглядаються для двох варіантів його оптимізованих параметрів при періодичному навантаженні. Також аналізується вплив характеристик пружності контактуючих поверхонь на ефективність демпфера. Показано, що в системі з більш важким демпфером та з його невеликою жорсткістю реалізуються коливальні режими з багатю складною динамікою. Проте такий демпфер виявився ефективнішим, особливо при м'якому ударі.

Табл. 6. Рис. 3. Бібліогр.24.

UDC 539.3

Lizunov P.P., Pogorelova O.S., Postnikova T.G.

Influence of stiffness parameters on vibro-impact damper dynamics//Strength of Materials and Theory of Structures: Scientific-and-technical collected articles. – K.: KNUBA. 2023. – Issue110. – P. 21-35.

The article studies the dynamic behavior of a low-mass vibro-impact damper, considered as a device for passive vibration control. Its design scheme corresponds to the scheme of single-sided vibro-impact nonlinear energy sink (SSVI NES), which is supposed to be used for effective vibrations attenuation under different transient loads, namely, impulsive, broadband, wind. Its dynamics and effectiveness strongly depends both on the damper own parameters and the external load parameters. We consider the response regimes and the damper efficiency for two options of its optimized parameters under periodic loading. The influence of the elasticity characteristics of the colliding surfaces on the damper effectiveness is also analyzed. We show that the modes with rich complex dynamics are implemented in a system with a heavier damper with low stiffness. Despite this, it is more effective, especially with a softer impact.

Табл. 6. Рис. 3. Бібліогр.24.

Автор (вчена ступень, вчене звання, посада): доктор технічних наук, професор, завідувач кафедри будівельної механіки КНУБА, директор НДІ будівельної механіки

ЛІЗУНОВ Петро Петрович

Адреса робоча: 03680 Україна, м. Київ, Повітрофлотський проспект 31, Київський національний університет будівництва і архітектури

Робочий тел.: +38(044) 245-48-29.

мобільний тел.: +38(067)921-70-05

Ім'я: lizunov@knuba.edu.ua

ORCID ID: <http://orcid.org/0000-0003-2924-3025>

Автор (вчена ступень, вчене звання, посада): кандидат фізико-математичних наук, старший науковий співробітник, провідний науковий співробітник НДІ будівельної механіки ПОГОРЕЛОВА Ольга Семенівна

Адреса робоча: 03680 Україна, м. Київ, Повітрофлотський проспект 31, Київський національний університет будівництва і архітектури

Робочий тел.: +38(044) 245-48-29

Мобільний тел.: +38(067) 606-03-00

Ім'я: pogosl3@ukr.net

ORCID ID: <http://orcid.org/0000-0002-5522-3995>

Автор (вчена ступень, вчене звання, посада): кандидат технічних наук, старший науковий співробітник, старший науковий співробітник НДІ будівельної механіки ПОСТНІКОВА Тетяна Георгіївна

Адреса робоча: 03680 Україна, м. Київ, Повітрофлотський проспект 31, Київський національний університет будівництва і архітектури

Робочий тел.: +38(044) 245-48-29

Мобільний тел.: +38(050) 353-47-19

Ім'я: postnikova.tg@knuba.edu.ua

ORCID ID: <https://orcid.org/0000-0002-6677-4127>